

DA-BEV: Unsupervised Domain Adaptation for Bird’s Eye View Perception

Kai Jiang^{1*}, Jiaxing Huang^{2*}, Weiyang Xie¹, Yunsong Li¹, Ling Shao³, Shijian Lu^{2†}

¹State Key Laboratory of Integrated Services Networks, Xidian University, Xi’an 710071, China

²S-lab, School of Computer Science and Engineering, Nanyang Technological University

³UCAS-Terminus AI Lab, University of Chinese Academy of Sciences, Beijing, China

kjiang_19@stu.xidian.edu.cn {Jiaxing.Huang, Shijian.Lu}@ntu.edu.sg

Abstract

Camera-only Bird’s Eye View (BEV) has demonstrated great potential in environment perception in a 3D space. However, most existing studies were conducted under a supervised setup which cannot scale well while handling various new data. Unsupervised domain adaptive BEV, which effective learning from various unlabelled target data, is far under-explored. In this work, we design DA-BEV, the first domain adaptive camera-only BEV framework that addresses domain adaptive BEV challenges by exploiting the complementary nature of image-view features and BEV features. DA-BEV introduces the idea of query into the domain adaptation framework to derive useful information from image-view and BEV features. It consists of two query-based designs, namely, query-based adversarial learning (QAL) and query-based self-training (QST), which exploits image-view features or BEV features to regularize the adaptation of the other. Extensive experiments show that DA-BEV achieves superior domain adaptive BEV perception performance consistently across multiple datasets and tasks such as 3D object detection and 3D scene segmentation.

1. Introduction

3D visual perception [32, 45] aims at sensing and understanding surrounding environments in 3D space, which plays an important role in various applications such as mobile robotics [3, 20], autonomous driving [61, 67], virtual reality [54, 82], etc. Despite the remarkable progress of monocular and LiDAR-based 3D perception [4, 11, 13, 19, 29, 35, 58, 60, 71, 75, 76, 85], camera-only 3D perception in Bird’s Eye View (BEV) [28, 37, 39, 40, 70, 73] has drawn increasing attention in recent years thanks to its advantages in comprehensive 3D understanding, rich semantic information, high computational efficiency, and low deployment

*These authors contributed equally to this work.

†Corresponding author.

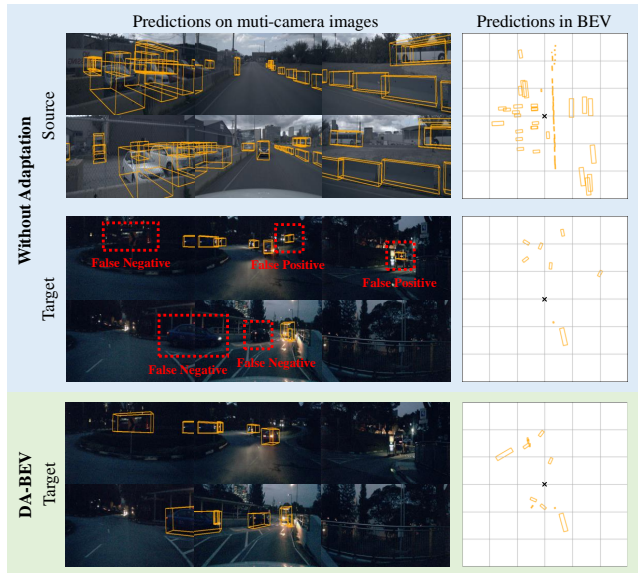


Figure 1. Domain adaptive bird’s eye view perception (DA-BEV). The first two rows show the detection by a source-only model (trained with source data with no adaptation) over a source scene and a target scene, respectively. The yellow 3D boxes indicate correct detection while the red dotted boxes highlight false-positive and false-negative detection. The third row shows the detection by our DA-BEV on the same target scene. The two columns visualize the 3D predictions in multi-camera view and bird’s eye view, respectively.

cost. On the other hand, camera-only BEV models [63] trained over a source domain usually experience clear performance degradation when applied on a target domain due to clear cross-domain discrepancy as illustrated in Fig. 1.

Unsupervised Domain adaptation (UDA) [68] aims to address the cross-domain discrepancy by transferring a deep network model trained over a labelled source domain towards an unlabelled target domain. It has been extensively explored for various 2D computer vision tasks [16, 46, 80, 84] that perceive environments in a 2D space. However,

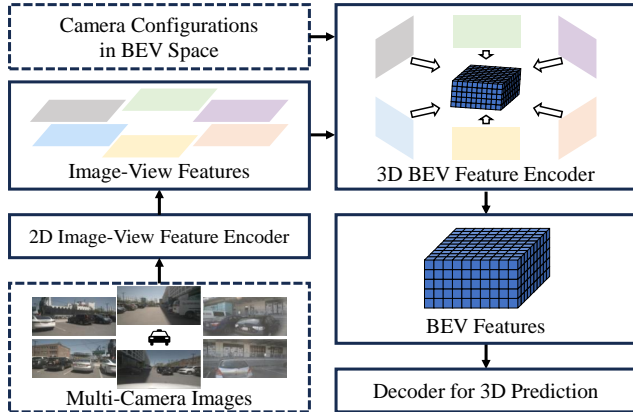


Figure 2. The architecture of camera-only BEV models. Boxes in dash lines denote model inputs including multi-camera images and camera configurations. Boxes in solid lines stand for encoding/decoding processes and intermediate representations.

how to mitigate the cross-domain discrepancy for camera-only BEV perception is much more challenging but largely under explored.

We explore unsupervised domain adaptation for camera-only BEV perception, and we start from a simple observation that camera-only BEV perception generally works in two stages by first encoding multi-camera images into image-view features and then fusing the image-view features with the corresponding camera configurations into BEV features. As shown in Fig. 2, the image-view features capture largely local information within each single-view image which suffer from similar inter-domain discrepancy as 2D images in traditional unsupervised domain adaptation. As a comparison, BEV features capture global 3D information from camera configurations within the BEV space which usually suffer from more severe inter-domain discrepancy due to explicit changes of camera configurations beyond the change of image styles and appearance within the image-view features. Hence, one effective way of bridging the inter-domain discrepancy of camera-only BEV perception is by exploiting the complementary nature of image-view features and BEV features.

To this end, we design DA-BEV, the first domain adaptive camera-only BEV perception framework that addresses BEV domain adaptation challenges by exploiting the complementary nature of image-view features and BEV features. We introduce learnable queries to facilitate the interplay between image-view and BEV features while adapting them across domains. Specifically, the global 3D information from BEV features helps adapt image-view features while the 2D information in image-view features with less domain variation helps adapt BEV features. Following this philosophy, we design two query-based domain adaptation techniques including query-based adversarial learn-

ing (QAL) and query-based self-training (QST): QAL/QST exploits the useful information queried from image-view features or BEV features to regularize the “adversarial learning”/“self-training” of the another.

The proposed DA-BEV has three desirable features: 1) It introduces a novel query-based domain adaptation strategy that exploits the complementary nature of image-view features and BEV features for unsupervised BEV perception adaptation. The query-based domain adaptation strategy is well aligned with the architecture of camera-only BEV perception models; 2) It designs query-based adversarial learning and query-based self-training that achieve UDA by aligning inter-domain features and maximizing the target-domain likelihood, respectively. The two designs complement each other which jointly achieve robust unsupervised BEV perception adaptation effectively; 3) It is generic and can work for different camera-only BEV perception tasks such as 3D object detection and 3D scene segmentation.

The contributions of this work can be summarized in three major aspects. *First*, we explore unsupervised camera-only BEV perception adaptation and propose a query-based technique that mitigates the inter-domain discrepancy by exploiting the complementary nature of image-view features and BEV features. To the best of our knowledge, this is the first work that exploits the specific BEV network architecture for unsupervised BEV perception adaptation. *Second*, we design DA-BEV that introduces query-based adversarial learning and query-based self-training that jointly tackle domain adaptive BEV perception effectively. *Third*, extensive experiments show that DA-BEV achieves superior BEV perception adaptation consistently across different datasets and tasks such as 3D object detection and 3D scene segmentation.

2. Related Work

2.1. Camera-only BEV Perception

Camera-only Bird’s Eye View (BEV) perception [32,45] has recently attracted increasing attention thanks to its rich semantic information, high computational efficiency, and low deployment cost. It captures multi-view images of a scene and formulates unified BEV feature in ego-car coordinates for various 3D vision tasks such as 3D detection, map segmentation, etc. According to the way of view transformation, most existing camera-only BEV methods can be grouped into four categories [45], namely, homograph-based, depth-based, multilayer perception (MLP)-based, and transformer-based. Homograph-based methods [17, 22, 43, 49, 56] directly transform the multi-view image features into BEV features with explicitly constructed homography matrices. The recent are computationally efficient but exhibit limited performance in complex real-world scenarios. Depth-based methods [2, 10, 24–

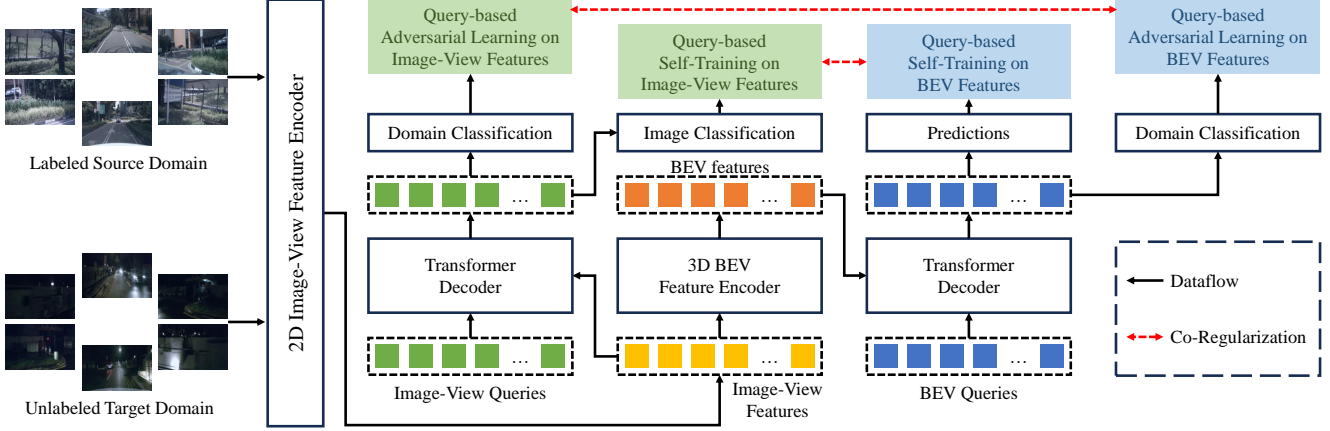


Figure 3. The overall framework of DA-BEV, which exploits the complementary nature of image-view and BEV features for unsupervised BEV perception adaptation. It comprises two designs including query-based adversarial learning (QAL) and query-based self-training (QST). The former exploits the useful information queried from image-view or BEV features to regularize the adversarial learning of the another, while the latter exploits the useful information queried from both image-view and BEV features to regularize their self-training.

[26, 34, 57, 64, 69, 81] estimate depth distribution and apply it to generate BEV features from multi-view 2D features. MLP methods [21, 33, 47, 50, 52, 74, 86] learn a transformation between multi-view features and BEV features, aiming to relieve the inherent inductive biases under a calibrated camera setup. The recent transformer-based methods [6, 8, 9, 12, 28, 37, 39, 40, 48, 51, 55, 62, 66, 70, 72, 73] design a set of BEV queries to retrieve the corresponding image features via cross-attention, ultimately constructing BEV features in a top-down manner. Differently, we explore unsupervised domain adaptation for camera-only BEV perception.

2.2. Domain Adaptation

Domain Adaptation aims to adapt source-trained models towards various target domains. Most existing work focuses on unsupervised domain adaptation (UDA) for 2D vision tasks, which minimizes the domain discrepancy by discrepancy minimization [41, 59], adversarial training [18, 44, 59], or self-training [30, 78, 79]. However, most existing 2D UDA methods do not work well in 3D vision tasks that aim to understand objects and scenes in three-dimensional space. 3D UDA has been explored recently. For example, STMono3D [36] introduces self-training for cross-domain monocular 3D object detection. [5, 53] and [1] exploit lidar and multimodal data in 3D UDA but they cannot work for camera-only BEV perception with extra data modality. Recently, M²ATS [38] studies domain adaptation for multi-view 3D detection but still relies on depth supervision from Lidar. Unsupervised domain adaptation has been largely neglected for the task of camera-only BEV perception

3. Domain Adaptive BEV Perception

3.1. Preliminary

Task definition. This work focuses on the task of unsupervised domain adaptation of camera-only BEV perception. It involves a labelled source domain $D_S = \{x_S^n, k_S^n, y_S^n\}_{n=1}^{N_S}$ and an unlabelled target domain $D^T = \{x_T^n, k_T^n\}_{n=1}^{N_T}$, where x denotes a set of multi-camera images, k stands for the camera configurations, and y denotes the 3D object annotations in the BEV space as represented by x and k . The goal is to learn a BEV perception model that performs well on the unlabelled target domain.

A Revisit of BEV Models. Camera-only BEV model typically works in two stages as illustrated in Fig. 2. It first encodes multi-camera images into image-view features and then fuses these image-view features with the corresponding camera configurations to produce BEV features for 3D perception. Specifically, camera-only BEV model consists of a 2D image-view feature encoder \mathcal{E}^{iv} , a 3D BEV feature encoder \mathcal{E}^{bev} , a BEV feature decoder \mathcal{D}^{bev} , and a 3D detection head \mathcal{H}_{det} . Given a set of multi-camera images x and their corresponding camera configurations k , camera-only BEV model first encodes x into image-view features with the \mathcal{E}^{iv} as follows:

$$f^{iv} = \mathcal{E}^{iv}(x), \quad (1)$$

The image features are then encoded with the corresponding camera configurations k into BEV features with the \mathcal{E}^{bev} :

$$f^{bev} = \mathcal{E}^{bev}(f^{iv}, k). \quad (2)$$

The BEV feature decoder \mathcal{D}^{bev} then decodes the BEV features f^{bev} with a set of learnable BEV queries q^{bev} :

$$\hat{q}^{bev} = \mathcal{D}^{bev}(q^{bev}, f^{bev}). \quad (3)$$

where the BEV queries q^{bev} interact with the BEV features f^{bev} and aggregate the 3D location information of objects in BEV, leading to the decoded query features \tilde{q}^{bev} . Given the decoded query features \tilde{q}^{bev} , 3D detection head \mathcal{H}_{det} predicts 3D object bounding boxes p^{det} by:

$$p^{det} = \mathcal{H}_{det}(\tilde{q}^{bev}). \quad (4)$$

Under the setting of supervised learning, the camera-only BEV model can be formulated as follows:

$$L^{bev} = \mathcal{L}_{det}(p^{det}, y). \quad (5)$$

where \mathcal{L}_{det} denotes a 3D detection loss function.

3.2. Framework of DA-BEV

Our method tackles BEV domain adaptation challenges by exploiting the complementary nature of image-view features and BEV features as illustrated in Fig. 3. Specifically, we design novel query-based domain adaptation that introduces learnable queries to enable interaction between the image-view and BEV features and as well as their synergetic adaptation. Intuitively, the global 3D information from BEV features helps adapt image-view features while the local 2D information in image-view features with less domain variation helps adapt BEV features. Based on this philosophy, we design two query-based domain adaptation techniques, namely, query-based adversarial learning (QAL) and query-based self-training (QST). QAL/QST exploits the useful information queried from image-view features or BEV features to regularize the “adversarial learning”/“self-training” of the another as illustrated in Fig. 3.

To capture 2D information in the image-view features with less inter-domain, we introduce an image-view feature decoder \mathcal{D}^{iv} with a set of learnable image-view queries q^{iv} . The interaction between q^{iv} f^{iv} thus produces the image-view query features \tilde{q}^{iv} as follows:

$$\tilde{q}^{iv} = \mathcal{D}^{iv}(q^{iv}, f^{iv}). \quad (6)$$

The query feature \tilde{q}^{iv} is then fed into a multi-label classification head \mathcal{H}_{cls} to predict the probability of each object category, where \mathcal{H}_{cls} is trained by a multi-label classification loss function L_{cls} as follows:

$$p^{cls} = \mathcal{H}_{cls}(\tilde{q}^{iv}), \quad L^{iv} = \mathcal{L}_{cls}(p^{cls}, y^{iv}), \quad (7)$$

where y^{iv} denotes the image-view multi-label classification annotations. Note \mathcal{L}_{cls} is computed for both source and target data. For source data x_S, k_S, y_S , we generate the image-view multi-label classification annotation y_S^{iv} by merging the object category labels in y_S . For target data x_T, k_T , we generate y_T^{iv} based on the model predictions as defined in Eq. 14.

Hence, the decoded image-view query features \tilde{q}^{iv} captures rich 2D semantic and location information from the image-view features. They contain much less inter-domain discrepancy than the BEV features and can therefore benefit BEV feature adaptation greatly. In addition, the multi-label classification training objective of image-view query q^{iv} encourages capturing more balanced information among different categories, which facilitates the adaptation of BEV feature which are trained with one-hot object category annotation and thus often suffer from clear class imbalance issues [14].

To capture the global 3D information in BEV features, we directly employ the off-the-shelf BEV queries q^{bev} in Eq. 3, which interact with BEV features to generate the decoded BEV query features \tilde{q}^{bev} . As BEV features are encoded with camera configurations and q^{bev} is trained with 3D object annotations, the decoded BEV query feature \tilde{q}^{bev} captures rich global 3D information including the object position in 3D BEV space. They can help the adaptation of image-view features that capture little global 3D information in BEV space.

3.3. Query-based Adversarial Learning

Our proposed QAL exploits the useful information queried from image-view or BEV features to regularize the adversarial learning of the another. As illustrated in Fig. 3, QAL employs two domain classifiers to measure the inter-domain distances of the image-view query features and the BEV query features respectively, and utilizes the measured inter-domain distance for mutual regularization.

Hence, QAL simultaneously mitigates the inter-domain discrepancies of the local 2D information in image-view features and the global 3D information in BEV features, both being critical to locate and recognize objects and backgrounds in a 3D space. Besides, the adversarial learning of 2D image-view query features involves little 3D information, where the BEV query features can regularize it effectively by providing rich global 3D information, i.e., enhancing 2D image-view adversarial learning for the samples with significant 3D BEV inter-domain discrepancies while diminishing 2D image-view adversarial learning for the samples with minor 3D BEV inter-domain discrepancies. Similarly, the adversarial learning of 3D BEV query features can be regularized by the image-view query features capturing rich 2D semantic and location information.

Specifically, we employ domain classifiers \mathcal{C}^{iv} and \mathcal{C}^{bev} to measure the inter-domain distance of 2D image-view and 3D BEV features as follows:

$$\begin{aligned} \lambda^{iv} &= \exp(-\log \mathcal{C}^{iv}(\tilde{q}_s^{iv}) - \log(1 - \mathcal{C}^{iv}(\tilde{q}_t^{iv}))), \\ \lambda^{bev} &= \exp(-\log \mathcal{C}^{bev}(\tilde{q}_s^{bev}) - \log(1 - \mathcal{C}^{bev}(\tilde{q}_t^{bev}))), \end{aligned} \quad (8)$$

where \tilde{q}_s^{iv} and \tilde{q}_t^{iv} denote the decoded image-view query features in Eq. (6) that interacted with the source and target

image-view features, respectively. \tilde{q}_s^{bev} and \tilde{q}_t^{bev} denote the decoded BEV query features in Eq. (3) that interacted with source and target domain BEV features, respectively.

The mutual regularization of QAL between image-view and BEV features can be formulated as follows,

$$L_{qal} = \lambda^{iv} \cdot \mathcal{L}_{al}(\tilde{q}_s^{iv}, \tilde{q}_t^{iv}) + \lambda^{bev} \cdot \mathcal{L}_{al}(\tilde{q}_s^{bev}, \tilde{q}_t^{bev}), \quad (9)$$

where $\mathcal{L}_{al}(\cdot)$ is a widely adopted adversarial learning loss function for cross-domain alignment [15].

3.4. Query-based Self-training

Our proposed QST exploits the useful information queried from both image-view and BEV features to regularize their self-training, as shown in Fig. 3. Intuitively, the decoded image-view query features capture rich 2D semantic and location information that has less inter-domain discrepancy, while the decoded BEV query features capture rich global 3D information in the BEV space. Hence, the two types of features complement each other and together regularize self-training effectively with comprehensive 2D and 3D information.

Specifically, QST first leverages the predictions from image-view or BEV features to denoise the predictions from the other:

$$\hat{p}^{cls} = \max(p^{det}) \cdot p^{cls}, \quad \hat{p}^{det} = p^{det} \cdot p^{cls}, \quad (10)$$

where p^{cls}/\hat{p}^{cls} and p^{det}/\hat{p}^{det} denotes image-view and BEV predictions before/after cross-view denoising. The operation $\max(\cdot)$ stands for selecting the maximum probability in BEV predictions for each category. Please note we conduct the above cross-view denoising operations for each camera perspective, respectively.

Then, QST acquires global class distribution by accumulating the denoised predictions that capture comprehensive 2D and 3D information, and further exploit it to facilitate pseudo label generation. Specifically, we model the global class probability distribution as Gaussian distributions $\mathcal{N}(\mu_c, \sigma_c^2)$, where c denotes the category index. We estimate $\hat{\mu}_c$ and $\hat{\sigma}_c^2$ by maintaining a first-in-first-out queue of historical predictions:

$$\hat{\mu}_c = \frac{1}{B} \sum_{j=1}^B \hat{p}_c^{det}(j), \quad \hat{\sigma}_c^2 = \frac{1}{B-1} \sum_{j=1}^B (\hat{p}_c^{det}(j) - \hat{\mu}_c)^2, \quad (11)$$

where B denotes the queue length and $\hat{p}_c^{det}(j)$ stands for the j -th historical prediction in the queue. Note we use \hat{p}^{det} only as it already includes the 2D information in \hat{p}^{cls} after cross-denoising.

We accumulate $\hat{\mu}_c$ and $\hat{\sigma}_c^2$ along the training process for more stable estimation of $\mathcal{N}(\mu_c, \sigma_c^2)$:

$$\mu_c = \gamma \cdot \mu_c + (1-\gamma) \cdot \hat{\mu}_c, \quad \sigma_c^2 = \gamma \cdot \sigma_c^2 + (1-\gamma) \cdot \hat{\sigma}_c^2, \quad (12)$$

where γ denotes the Exponential Moving Average parameter for smooth update.

According to the estimated global class probability distribution, we select the top v percent predictions as the pseudo labels for each category. The pseudo label threshold τ_c can be determined by solving the following equation:

$$\frac{\Phi(1|\mu_c, \sigma_c) - \Phi(\tau_c|\mu_c, \sigma_c)}{\Phi(1|\mu_c, \sigma_c) - \Phi(0|\mu_c, \sigma_c)} = v, \quad (13)$$

where $\Phi(\cdot)$ refers to the cumulative density function of $\mathcal{N}(\mu_c, \sigma_c^2)$. Note we apply thresholds $\{\tau_c|c = 1, \dots, C\}$ to both image-view and BEV predictions \hat{p}^{cls} and \hat{p}^{det} to acquire image-view and BEV pseudo labels \hat{y}^{cls} and \hat{y}^{det} .

Our pseudo label generation method thus has three desirable features: 1) the thresholds are update-to-date as they are dynamically determined along the training process according to the complementary 2D and 3D information captured by image-view and BEV features; 2) it mitigates class imbalance issue by selecting the same percentage of pseudo labels for each class; 3) it works online and does not need an additional inference round as in [27, 87].

The training loss of QST can thus be formulated by:

$$L_{qst} = \mathcal{L}_{cls}(p^{cls}, \hat{y}^{iv}) + \mathcal{L}_{det}(p^{det}, \hat{y}^{bev}). \quad (14)$$

3.5. Overall objective

In summary, the overall training objective of the proposed DA-BEV can be formulated as follows:

$$\min_{\mathcal{E}, \mathcal{D}, \mathcal{H}} \max_c L^{iv} + L^{bev} + L_{qst} + L_{qal}, \quad (15)$$

where $\mathcal{E} = \{\mathcal{E}^{2d}, \mathcal{E}^{3d}\}$, $\mathcal{D} = \{\mathcal{D}^{iv}, \mathcal{D}^{bev}\}$, $\mathcal{H} = \{\mathcal{H}_{cls}, \mathcal{H}_{det}\}$, $\mathcal{C} = \{\mathcal{C}^{iv}, \mathcal{C}^{bev}\}$.

4. Experiments

4.1. Datasets

We benchmark our DA-BEV extensively over various BEV adaptation scenarios including adaptation across different illumination conditions, different weather conditions, different cities, and different Camera systems. The four BEV adaptation scenarios involve two 3D perception datasets including nuScenes [7] and Lyft [23].

nuScenes [7] is a large-scale autonomous driving 3D dataset, which comprises 6-camera images captured from 1000 scenes, including the scenes with daytime/nighttime and ‘‘clear weather’’/‘‘rainy weather’’ conditions, and from Singapore/Boston cities. For 3D object detection, it includes 1.4M annotated 3D bounding boxes with 10 categories. For 3D scene segmentation [40, 83], it contains 200K frames with fine-grained segmentation annotations in 3D space.

Daytime → Nighttime												
Methods	Average Precision \uparrow										mAP \uparrow	NDS \uparrow
	Car	Truck	Cons. Vehicle	Bus	Trailer	Barrier	Motorcycle	Bicycle	Pedestrian	Cone		
Source Only	40.79	28.88	0.41	29.71	0.00	9.15	22.00	0.71	24.66	2.84	15.92	22.44
SFA [65]	40.70	27.05	0.00	30.48	0.00	11.04	21.52	0.42	24.21	4.69	16.01	23.95
MTTrans [77]	41.48	34.39	0.01	30.49	0.00	12.48	21.40	0.69	24.94	4.16	17.00	24.48
STM3D [36]	41.77	33.19	0.27	29.22	0.00	13.28	21.94	0.28	24.21	4.36	16.85	24.41
DA-BEV (Ours)	45.07	41.96	1.91	38.12	0.00	16.66	25.74	0.54	28.05	4.65	20.27	26.98

Table 1. Unsupervised domain adaptation of camera-only BEV perception across different illumination conditions.

Clear Weather → Rainy Weather												
Methods	Average Precision \uparrow										mAP \uparrow	NDS \uparrow
	Car	Truck	Cons. Vehicle	Bus	Trailer	Barrier	Motorcycle	Bicycle	Pedestrian	Cone		
Source Only	41.68	18.19	2.24	41.58	7.07	38.09	13.16	21.57	33.31	30.66	24.75	32.84
SFA [65]	42.23	18.87	2.12	49.21	6.26	37.61	11.11	21.59	33.09	31.78	25.39	33.18
MTTrans [77]	41.04	20.08	3.51	50.42	7.07	37.78	11.56	20.91	33.57	34.08	26.00	33.68
STM3D [36]	42.45	19.22	2.68	47.62	7.00	38.52	13.39	21.44	33.85	31.97	25.81	33.56
DA-BEV (Ours)	46.72	25.06	3.38	51.62	8.70	46.65	17.46	26.85	39.37	37.80	30.36	36.81

Table 2. Unsupervised domain adaptation of camera-only BEV perception across different weather conditions.

Singapore → Boston												
Method	Average Precision \uparrow										mAP \uparrow	NDS \uparrow
	Car	Truck	Cons. Vehicle	Bus	Trailer	Barrier	Motorcycle	Bicycle	Pedestrian	Cone		
Source Only	41.29	8.51	0.00	29.84	0.00	11.23	4.06	5.80	28.59	35.80	16.51	21.74
SFA [65]	42.75	10.51	0.00	29.25	0.00	12.78	3.68	8.43	31.70	37.04	17.61	23.43
MTTrans [77]	42.68	11.24	0.00	29.97	0.00	13.91	3.42	8.60	32.56	38.01	18.04	24.69
STM3D [36]	43.44	10.69	0.00	28.29	0.00	13.03	3.83	8.75	32.60	39.50	18.01	24.68
DA-BEV (Ours)	45.35	14.69	0.00	31.68	0.00	19.58	6.63	9.78	34.20	42.12	20.40	28.35

Table 3. Unsupervised domain adaptation results of camera-only BEV perception across different cities.

Lyft [23] is a self-driving dataset for 3D perception, which has a diverse set of cameras with distinct intrinsic and extrinsic parameters. It comprises 366 scenes with 1.3M 3D object detection annotations, which are captured from California, and under a different camera system as compared with nuScenes.

With nuScenes [7] and Lyft [23], the four BEV adaptation scenarios are formulated as: “nuScenes Daytime → nuScenes Nighttime” for cross-illumination adaptation, “nuScenes clear weather → nuScenes rainy weather” for cross-weather adaptation, “nuScenes Singapore → nuScenes Boston” for cross-city adaptation and “Lyft camera systems → nuScenes camera systems” for adaptation across different camera configurations.

4.2. Implementation Details

We implement our DA-BEV upon PETR [39] with backbone VoVNetV2 [31]. Following PETR, we adopt AdamW [42] optimizer with an initial learning rate of 1×10^{-4} and a weight decay of 0.01. All models are trained for 50k iterations on one 2080Ti GPU with a batch size of 2. For 3D object detection, the transformer decoder consist of 6 layers with 900 object queries. For 3D scene segmenta-

tion, we follow the settings in [40, 83], where 625 segmentation queries along with a 6 layer transformer decoder are adopted for semantic segmentation result.

4.3. Main Results

Since there is little study on domain adaptive camera-only BEV, we compare our method with a number of domain adaptation methods that achieved state-of-the-art performance in 2D object detection [65, 77] and monocular 3D object detection [36].

These compared methods can be easily applied on domain adaptive camera-only BEV perception by directly introducing their adversarial learning and/or self-training techniques into camera-only BEV perception model. The comparisons are conducted over four challenging BEV adaptation scenarios as detailed in the following text.

Tables 1, 2 and 3 report unsupervised domain adaptation of camera-only BEV perception across different illuminations, weathers and cities, respectively. We can observe that DA-BEV achieves substantial improvements upon the baseline on these three adaptation scenarios, including 4.35%, 5.61% and 4.18% improvements in mAP, and 4.54%, 3.97% and 6.61% improvement in NDS. In

Lyft Camera Systems \rightarrow nuScenes Camera Systems								
Methods	Average Precision \uparrow						mAP \uparrow	NDS* \uparrow
	Car	Truck	Bus	Motorcycle	Bicycle	Pedestrian		
Source Only	28.43	3.70	4.30	12.88	0.65	10.15	10.02	16.44
SFA [65]	33.17	3.55	4.18	12.44	0.62	11.96	10.98	17.87
MTTrans [77]	33.19	3.98	4.00	13.03	0.75	11.06	11.00	17.98
STM3D [36]	36.51	4.34	4.63	15.96	0.51	14.93	12.81	18.58
DA-BEV (Ours)	38.45	3.93	4.23	23.53	0.75	22.85	15.62	24.78

Table 4. Unsupervised domain adaptation of camera-only BEV perception across different camera systems.

Methods	QAL			QST			mAP \uparrow	NDS \uparrow
	Image-View	BEV	Co-Regularization	Image-View	BEV	Co-Regularization		
Source Only	-	-	-	-	-	-	15.93	22.41
DA-BEV	✓						16.45	22.93
	✓	✓					16.96	23.21
	✓	✓	✓				17.80	24.07
	✓	✓	✓	✓			18.53	25.06
	✓	✓	✓	✓	✓		19.39	26.30
	✓	✓	✓	✓	✓	✓	20.27	26.98

Table 5. Ablation study of the proposed DA-BEV. The experiments are conducted on Daytime \rightarrow Nighttime adaptation.

Method	IoU			mIoU
	Drive	Lane	Vehicle	
Source Only	39.33	25.91	18.78	28.01
DA-BEV (Ours)	51.37	30.43	24.98	35.59

Table 6. Camera-only BEV perception of 3D scene segmentation on Daytime \rightarrow Nighttime domain adaptation.

addition, DA-BEV outperforms the state-of-the-art UDA methods clearly and consistently across these three adaptation scenarios. The superior BEV adaptation performance of DA-BEV is largely attributed to two factors: 1) DA-BEV introduces query-based domain adaptation that ingeniously exploits the complementary nature of image-view features and BEV features in BEV model, which helps tackle the domain gaps in BEV perception effectively. 2) DA-BEV introduces two query-based domain adaptation methods, i.e., QAL and QST, which complement each other and jointly achieve robust BEV perception adaptation effectively.

Table 4 reports unsupervised domain adaptation of camera-only BEV perception across different camera systems. Lyft and nuScenes data are collected with very different camera systems that have clear domain gaps in terms of camera intrinsic parameters including camera focal lengths and FOVs as well as camera extrinsic parameters such as camera poses and camera positions. It can be observed that DA-BEV outperforms both the baseline and state-of-the-art UDA methods substantially and consistently in mAP and NDC metrics, including over 3.98% improvements in mAP and 7.31% improvements in NDS. These experiments demonstrate that DA-BEV can well handle the BEV adaptation across different camera systems that suffers from severe domain gaps from camera configuration

inputs beyond those from image inputs.

4.4. Ablation Study

We conduct extensive ablation studies to investigate how different components in DA-BEV contribute. The experiments are conducted on Daytime \rightarrow Nighttime adaptation. As Table 5 shows, *the baseline* does not perform well due to the domain gaps. As a comparison, including query-based adversarial learning on image-view features and/or BEV features improves the baseline clearly, indicating that QAL can simultaneously mitigate the inter-domain discrepancies in both 2D image-view features and 3D BEV features. In addition, introducing co-regularization between image-view and BEV query-based adversarial learning further improves the performance clearly, showing that image-view and BEV features encode complementary cross-domain discrepancy information that effectively regularize the adversarial learning of each other.

In addition, applying query-based self-training on image-view and/or BEV features brings clear improvements, indicating that QST helps learn effective 2D and 3D information of unlabeled target data from image-view and BEV, respectively. Moreover, the co-regularization of query-based self-training of image-view and BEV features brings further improvement, demonstrating that image-view and BEV features provide complementary and comprehensive target information that effectively regularizes their self-training. Further, the combination of QAL and QST performs the best clearly, showing that QAL and QST complement each other and jointly achieve robust unsupervised BEV perception adaptation effectively.

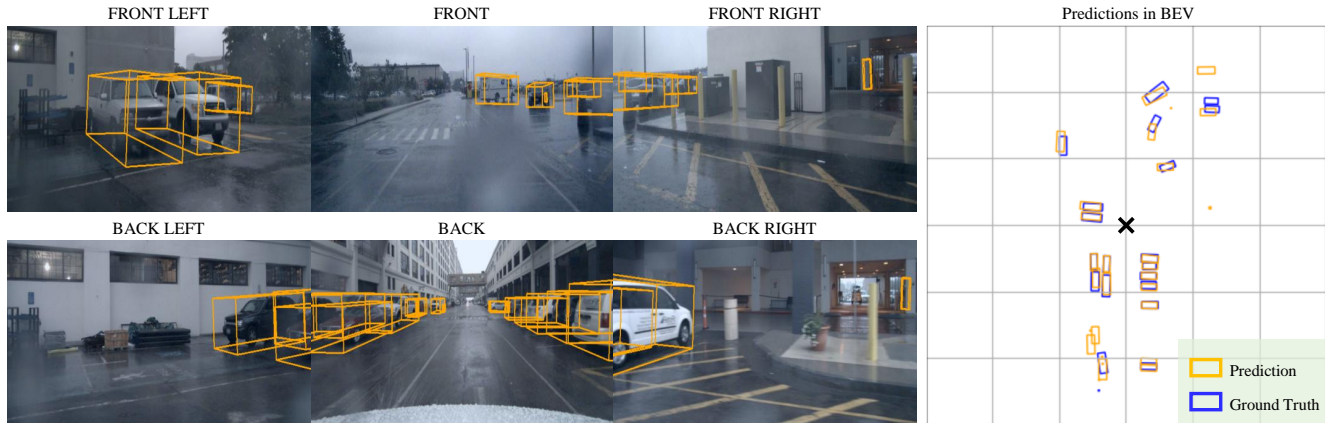


Figure 4. Qualitative illustration of DA-BEV on 3D object detection for cross-weather domain adaptation (i.e., Clear Weather \rightarrow Rainy Weather). The left and right parts visualize the 3D predictions in multi-camera view and bird’s eye view, respectively.

v	10%	15%	20%	25%	30%
mAP	18.24	19.83	20.27	20.15	19.57
γ	0.9	0.99	0.999	0.9999	0.99999
mAP	17.20	20.03	20.27	19.48	18.86

Table 7. Parameter analysis on Daytime \rightarrow Nighttime adaptation.

4.5. Discussion

Generalization across 3D perception tasks. We study how DA-BEV generalizes across 3D perception tasks by evaluating it over two representative tasks including 3D object detection and 3D scene segmentation. Experiments in Tables 1-4 and 6 show that DA-BEV achieves superior performance consistently over 3D detection and segmentation tasks, demonstrating the generalization ability of DA-BEV across different 3D perception tasks.

Parameter studies. As defined in Eq. 13 parameter v controls how many predictions we select as the pseudo labels. We study v by changing it from 10% to 30% with a step of 5%. The experiments in the top part of Table 7 show that v does not affect domain adaptation much while it changes from 15% to 30%. The performance drops more when v is set as 10%, largely because the adaptation is biased toward the source when very limited pseudo labels of target samples are selected. As mentioned in Eq. 12, parameter γ controls the update speed of the estimated global class probability distribution. We study γ by changing it from 0.9 to 0.99999. The experiments in the bottom part of Table 7 show that DA-BEV is tolerant to parameter γ when it varies from 0.99 to 0.9999. The performance drops more when γ is set as 0.9 or 0.99999, largely because these two values lead to too fast or too slow update, resulting in unstable or nearly fixed estimation of global class probability distribution and degraded performance.

Backbone		R50-C5	R50-P4	VoV-P4
Source Only	mAP	10.63	11.61	15.93
DA-BEV (Ours)	mAP	13.03	14.22	20.27

Table 8. Generalization across network backbones.

Generalization across network backbones. We study how DA-BEV generalizes across network backbones by evaluating it over three backbones of different sizes, including ResNet-50-C5 (46.9M), ResNet-50-P4 (46.9M) and VoV-P4 (96.9M). Results in Table 8 show that DA-BEV improves consistently over both small and large backbones, demonstrating the generalization ability of DA-BEV across different network backbones.

Qualitative results. We provide qualitative illustrations of DA-BEV on cross-weather domain adaptation. As Fig. 4 shows DA-BEV can produce accurate 3D object detection under weather-induced domain gaps. For example, the left-most car in Front Left camera becomes fuzzy due to rains and our DA-BEV can still detect it accurately.

Due to the space limit, we provide more discussion and additional qualitative illustrations in the Appendix.

5. Conclusion

In this paper, we present DA-BEV, the first domain adaptive camera-only BEV framework that addresses domain adaptive BEV challenges by exploiting the complementary nature of image-view features and BEV features. DA-BEV introduces query-based adversarial learning (QAL) and query-based self-training (QST), where QAL/QST exploits the useful information queried from image-view features or BEV features to regularize the “adversarial learning”/“self-training” of the another. Extensive experiments showcase the superior domain adaptive BEV perception performance

of DA-BEV across various datasets and tasks. Moving forward, we will further explore the complementary nature of image-view and BEV features by introducing the temporal information of them.

References

- [1] David Acuna, Jonah Philion, and Sanja Fidler. Towards optimal strategies for training self-driving perception models in simulation. *Advances in Neural Information Processing Systems*, 34:1686–1699, 2021. [3](#)
- [2] Adil Kaan Akan and Fatma Güney. Stretchbev: Stretching future instance prediction spatially and temporally. In *European Conference on Computer Vision*, pages 444–460. Springer, 2022. [2](#)
- [3] Morris Antonello, Marco Carraro, Marco Pierobon, and Emanuele Menegatti. Fast and robust detection of fallen people from a mobile robot. In *2017 IEEE/RSJ international conference on intelligent robots and systems (IROS)*, pages 4159–4166. IEEE, 2017. [1](#)
- [4] Xuyang Bai, Zeyu Hu, Xinge Zhu, Qingqiu Huang, Yilun Chen, Hongbo Fu, and Chiew-Lan Tai. Transfusion: Robust lidar-camera fusion for 3d object detection with transformers. In *Proceedings of the IEEE/CVF conference on computer vision and pattern recognition*, pages 1090–1099, 2022. [1](#)
- [5] Alejandro Barrera, Jorge Beltrán, Carlos Guindel, Jose Antonio Iglesias, and Fernando García. Cycle and semantic consistent adversarial domain adaptation for reducing simulation-to-real domain shift in lidar bird’s eye view. In *2021 IEEE International Intelligent Transportation Systems Conference (ITSC)*, pages 3081–3086. IEEE, 2021. [3](#)
- [6] Florent Bartoccioni, Éloi Zablocki, Andrei Bursuc, Patrick Pérez, Matthieu Cord, and Karteek Alahari. Lara: Latents and rays for multi-camera bird’s-eye-view semantic segmentation. In *Conference on Robot Learning*, pages 1663–1672. PMLR, 2023. [3](#)
- [7] Holger Caesar, Varun Bankiti, Alex H Lang, Sourabh Vora, Venice Erin Liong, Qiang Xu, Anush Krishnan, Yu Pan, Giancarlo Baldan, and Oscar Beijbom. nuscenes: A multi-modal dataset for autonomous driving. In *Proceedings of the IEEE/CVF conference on computer vision and pattern recognition*, pages 11621–11631, 2020. [5](#), [6](#)
- [8] Li Chen, Chonghao Sima, Yang Li, Zehan Zheng, Jiajie Xu, Xiangwei Geng, Hongyang Li, Conghui He, Jianping Shi, Yu Qiao, et al. Persformer: 3d lane detection via perspective transformer and the openlane benchmark. In *European Conference on Computer Vision*, pages 550–567. Springer, 2022. [3](#)
- [9] Shaoyu Chen, Xinggang Wang, Tianheng Cheng, Qian Zhang, Chang Huang, and Wenyu Liu. Polar parametrization for vision-based surround-view 3d detection. *arXiv preprint arXiv:2206.10965*, 2022. [3](#)
- [10] Yilun Chen, Shu Liu, Xiaoyong Shen, and Jiaya Jia. Dsgn: Deep stereo geometry network for 3d object detection. In *Proceedings of the IEEE/CVF conference on computer vision and pattern recognition*, pages 12536–12545, 2020. [2](#)
- [11] Zehui Chen, Zhenyu Li, Shiquan Zhang, Liangji Fang, Qin-hong Jiang, and Feng Zhao. Autoalignv2: Deformable feature aggregation for dynamic multi-modal 3d object detection. *arXiv preprint arXiv:2207.10316*, 2022. [1](#)
- [12] Zehui Chen, Zhenyu Li, Shiquan Zhang, Liangji Fang, Qin-hong Jiang, and Feng Zhao. Graph-detr3d: rethinking overlapping regions for multi-view 3d object detection. In *Proceedings of the 30th ACM International Conference on Multimedia*, pages 5999–6008, 2022. [3](#)
- [13] Zehui Chen, Zhenyu Li, Shiquan Zhang, Liangji Fang, Qinghong Jiang, Feng Zhao, Bolei Zhou, and Hang Zhao. Autoalign: pixel-instance feature aggregation for multi-modal 3d object detection. *arXiv preprint arXiv:2201.06493*, 2022. [1](#)
- [14] Zhuoxiao Chen, Yadan Luo, Zheng Wang, Mahsa Baktashmotlagh, and Zi Huang. Revisiting domain-adaptive 3d object detection by reliable, diverse and class-balanced pseudo-labeling. In *Proceedings of the IEEE/CVF International Conference on Computer Vision*, pages 3714–3726, 2023. [4](#)
- [15] Yaroslav Ganin, Evgeniya Ustinova, Hana Ajakan, Pascal Germain, Hugo Larochelle, François Laviolette, Mario Marchand, and Victor Lempitsky. Domain-adversarial training of neural networks. *The journal of machine learning research*, 17(1):2096–2030, 2016. [5](#)
- [16] Zhiqiang Gao, Kaizhu Huang, Rui Zhang, Dawei Liu, and Jieming Ma. Towards better robustness against common corruptions for unsupervised domain adaptation. In *Proceedings of the IEEE/CVF International Conference on Computer Vision (ICCV)*, pages 18882–18893, October 2023. [1](#)
- [17] Noa Garnett, Rafi Cohen, Tomer Pe’er, Roei Lahav, and Dan Levi. 3d-lanenet: end-to-end 3d multiple lane detection. In *Proceedings of the IEEE/CVF International Conference on Computer Vision*, pages 2921–2930, 2019. [2](#)
- [18] Rui Gong, Wen Li, Yuhua Chen, and Luc Van Gool. Dlow: Domain flow for adaptation and generalization. In *Proceedings of the IEEE/CVF conference on computer vision and pattern recognition*, pages 2477–2486, 2019. [3](#)
- [19] Xiaoyang Guo, Shaoshuai Shi, Xiaogang Wang, and Hongsheng Li. Liga-stereo: Learning lidar geometry aware representations for stereo-based 3d detector. In *Proceedings of the IEEE/CVF International Conference on Computer Vision*, pages 3153–3163, 2021. [1](#)
- [20] Jens-Steffen Gutmann, Masaki Fukuchi, and Masahiro Fujita. 3d perception and environment map generation for humanoid robot navigation. *The International Journal of Robotics Research*, 27(10):1117–1134, 2008. [1](#)
- [21] Noureldin Hendy, Cooper Sloan, Feng Tian, Pengfei Duan, Nick Charchut, Yuesong Xie, Chuang Wang, and James Philbin. Fishing net: Future inference of semantic heatmaps in grids. *arXiv preprint arXiv:2006.09917*, 2020. [3](#)
- [22] Yunzhong Hou, Liang Zheng, and Stephen Gould. Multi-view detection with feature perspective transformation. In *Computer Vision—ECCV 2020: 16th European Conference, Glasgow, UK, August 23–28, 2020, Proceedings, Part VII 16*, pages 1–18. Springer, 2020. [2](#)
- [23] John Houston, Guido Zuidhof, Luca Bergamini, Yawei Ye, Long Chen, Ashesh Jain, Sammy Omari, Vladimir

- Iglovikov, and Peter Ondruska. One thousand and one hours: Self-driving motion prediction dataset. In *Conference on Robot Learning*, pages 409–418. PMLR, 2021. 5, 6
- [24] Anthony Hu, Zak Murez, Nikhil Mohan, Sofia Dudas, Jeffrey Hawke, Vijay Badrinarayanan, Roberto Cipolla, and Alex Kendall. Fiery: Future instance prediction in bird’s-eye view from surround monocular cameras. In *Proceedings of the IEEE/CVF International Conference on Computer Vision*, pages 15273–15282, 2021. 2
- [25] Junjie Huang and Guan Huang. Bevdet4d: Exploit temporal cues in multi-camera 3d object detection. *arXiv preprint arXiv:2203.17054*, 2022. 2
- [26] Junjie Huang, Guan Huang, Zheng Zhu, Yun Ye, and Dalong Du. Bevdet: High-performance multi-camera 3d object detection in bird-eye-view. *arXiv preprint arXiv:2112.11790*, 2021. 2
- [27] Muhammad Abdullah Jamal, Matthew Brown, Ming-Hsuan Yang, Liqiang Wang, and Boqing Gong. Rethinking class-balanced methods for long-tailed visual recognition from a domain adaptation perspective. In *Proceedings of the IEEE/CVF Conference on Computer Vision and Pattern Recognition*, pages 7610–7619, 2020. 5
- [28] Yanqin Jiang, Li Zhang, Zhenwei Miao, Xiatian Zhu, Jin Gao, Weiming Hu, and Yu-Gang Jiang. Polarformer: Multi-camera 3d object detection with polar transformer. In *Proceedings of the AAAI Conference on Artificial Intelligence*, volume 37, pages 1042–1050, 2023. 1, 3
- [29] Yang Jiao, Zequn Jie, Shaoxiang Chen, Jingjing Chen, Lin Ma, and Yu-Gang Jiang. Msmdfusion: Fusing lidar and camera at multiple scales with multi-depth seeds for 3d object detection. In *Proceedings of the IEEE/CVF Conference on Computer Vision and Pattern Recognition*, pages 21643–21652, 2023. 1
- [30] Dong-Hyun Lee. Pseudo-label: The simple and efficient semi-supervised learning method for deep neural networks. In *Workshop on Challenges in Representation Learning, ICML*, volume 3, page 2, 2013. 3
- [31] Youngwan Lee and Jongyoul Park. Centermask: Real-time anchor-free instance segmentation. In *Proceedings of the IEEE/CVF conference on computer vision and pattern recognition*, pages 13906–13915, 2020. 6
- [32] Hongyang Li, Chonghao Sima, Jifeng Dai, Wenhai Wang, Lewei Lu, Huijie Wang, Enze Xie, Zhiqi Li, Hanming Deng, Hao Tian, et al. Delving into the devils of bird’s-eye-view perception: A review, evaluation and recipe. *arXiv preprint arXiv:2209.05324*, 2022. 1, 2
- [33] Qi Li, Yue Wang, Yilun Wang, and Hang Zhao. Hdmapnet: An online hd map construction and evaluation framework. In *2022 International Conference on Robotics and Automation (ICRA)*, pages 4628–4634. IEEE, 2022. 3
- [34] Yin hao Li, Zheng Ge, Guanyi Yu, Jinrong Yang, Zengran Wang, Yukang Shi, Jianjian Sun, and Zeming Li. Bevdepth: Acquisition of reliable depth for multi-view 3d object detection. In *Proceedings of the AAAI Conference on Artificial Intelligence*, volume 37, pages 1477–1485, 2023. 2
- [35] Yingwei Li, Adams Wei Yu, Tianjian Meng, Ben Caine, Jiquan Ngiam, Daiyi Peng, Junyang Shen, Yifeng Lu, Denny Zhou, Quoc V Le, et al. Deepfusion: Lidar-camera deep fusion for multi-modal 3d object detection. In *Proceedings of the IEEE/CVF Conference on Computer Vision and Pattern Recognition*, pages 17182–17191, 2022. 1
- [36] Zhenyu Li, Zehui Chen, Ang Li, Liangji Fang, Qin hong Jiang, Xianming Liu, and Junjun Jiang. Unsupervised domain adaptation for monocular 3d object detection via self-training. In *European Conference on Computer Vision*, pages 245–262. Springer, 2022. 3, 6, 7
- [37] Zhiqi Li, Wenhai Wang, Hongyang Li, Enze Xie, Chonghao Sima, Tong Lu, Yu Qiao, and Jifeng Dai. Bevformer: Learning bird’s-eye-view representation from multi-camera images via spatiotemporal transformers. In *European conference on computer vision*, pages 1–18. Springer, 2022. 1, 3
- [38] Jiaming Liu, Rongyu Zhang, Xiaowei Chi, Xiaoqi Li, Ming Lu, Yandong Guo, and Shanghang Zhang. Multi-latent space alignments for unsupervised domain adaptation in multi-view 3d object detection. *arXiv preprint arXiv:2211.17126*, 2022. 3
- [39] Yingfei Liu, Tiancai Wang, Xiangyu Zhang, and Jian Sun. Petr: Position embedding transformation for multi-view 3d object detection. In *European Conference on Computer Vision*, pages 531–548. Springer, 2022. 1, 3, 6
- [40] Yingfei Liu, Junjie Yan, Fan Jia, Shuailin Li, Aqi Gao, Tiancai Wang, and Xiangyu Zhang. Petr2: A unified framework for 3d perception from multi-camera images. In *Proceedings of the IEEE/CVF International Conference on Computer Vision*, pages 3262–3272, 2023. 1, 3, 5, 6
- [41] Mingsheng Long, Yue Cao, Jianmin Wang, and Michael Jordan. Learning transferable features with deep adaptation networks. In *International Conference on Machine Learning*, pages 97–105, 2015. 3
- [42] Ilya Loshchilov and Frank Hutter. Decoupled weight decay regularization. *arXiv preprint arXiv:1711.05101*, 2017. 6
- [43] Abdelhak Loukkal, Yves Grandvalet, Tom Drummond, and You Li. Driving among flatmobiles: Bird-eye-view occupancy grids from a monocular camera for holistic trajectory planning. In *Proceedings of the IEEE/CVF Winter Conference on Applications of Computer Vision*, pages 51–60, 2021. 2
- [44] Yawei Luo, Ping Liu, Liang Zheng, Tao Guan, Junqing Yu, and Yi Yang. Category-level adversarial adaptation for semantic segmentation using purified features. *IEEE Transactions on Pattern Analysis and Machine Intelligence*, 44(8):3940–3956, 2021. 3
- [45] Yuexin Ma, Tai Wang, Xuyang Bai, Huitong Yang, Yue nan Hou, Yaming Wang, Yu Qiao, Ruigang Yang, Dinesh Manocha, and Xinge Zhu. Vision-centric bev perception: A survey. *arXiv preprint arXiv:2208.02797*, 2022. 1, 2
- [46] Poojan Oza, Vishwanath A Sindagi, Vibashan Vishnukumar Sharmini, and Vishal M Patel. Unsupervised domain adaptation of object detectors: A survey. *IEEE Transactions on Pattern Analysis and Machine Intelligence*, 2023. 1
- [47] Bowen Pan, Jiankai Sun, Ho Yin Tiga Leung, Alex Andonian, and Bolei Zhou. Cross-view semantic segmentation for sensing surroundings. *IEEE Robotics and Automation Letters*, 5(3):4867–4873, 2020. 3

- [48] Lang Peng, Zhirong Chen, Zhangjie Fu, Pengpeng Liang, and Erkang Cheng. Bevsegformer: Bird’s eye view semantic segmentation from arbitrary camera rigs. In *Proceedings of the IEEE/CVF Winter Conference on Applications of Computer Vision*, pages 5935–5943, 2023. 3
- [49] Lennart Reiher, Bastian Lampe, and Lutz Eckstein. A sim2real deep learning approach for the transformation of images from multiple vehicle-mounted cameras to a semantically segmented image in bird’s eye view. In *2020 IEEE 23rd International Conference on Intelligent Transportation Systems (ITSC)*, pages 1–7. IEEE, 2020. 2
- [50] Thomas Roddick and Roberto Cipolla. Predicting semantic map representations from images using pyramid occupancy networks. In *Proceedings of the IEEE/CVF Conference on Computer Vision and Pattern Recognition*, pages 11138–11147, 2020. 3
- [51] Wonseok Roh, Gysam Chang, Seokha Moon, Giljoo Nam, Chanyoung Kim, Younghyun Kim, Jinkyu Kim, and Sangpil Kim. Ora3d: Overlap region aware multi-view 3d object detection. *arXiv preprint arXiv:2207.00865*, 2022. 3
- [52] Avishkar Saha, Oscar Mendez, Chris Russell, and Richard Bowden. Enabling spatio-temporal aggregation in birds-eye-view vehicle estimation. In *2021 IEEE International Conference on Robotics and Automation (ICRA)*, pages 5133–5139. IEEE, 2021. 3
- [53] Khaled Saleh, Ahmed Abobakr, Mohammed Attia, Julie Iskander, Darius Nahavandi, Mohammed Hossny, and Saeid Nahvandi. Domain adaptation for vehicle detection from bird’s eye view lidar point cloud data. In *Proceedings of the IEEE/CVF International Conference on Computer Vision Workshops*, pages 0–0, 2019. 3
- [54] Martijn J Schuemie, Peter Van Der Straaten, Merel Krijn, and Charles APG Van Der Mast. Research on presence in virtual reality: A survey. *Cyberpsychology & behavior*, 4(2):183–201, 2001. 1
- [55] Yining Shi, Jingyan Shen, Yifan Sun, Yunlong Wang, Jiaxin Li, Shiqi Sun, Kun Jiang, and Diange Yang. Srcn3d: Sparse r-cnn 3d surround-view camera object detection and tracking for autonomous driving. *arXiv preprint arXiv:2206.14451*, 2022. 3
- [56] Liangchen Song, Jialian Wu, Ming Yang, Qian Zhang, Yuan Li, and Junsong Yuan. Stacked homography transformations for multi-view pedestrian detection. In *Proceedings of the IEEE/CVF International Conference on Computer Vision*, pages 6049–6057, 2021. 2
- [57] Yu Sun, Wu Liu, Qian Bao, Yili Fu, Tao Mei, and Michael J Black. Putting people in their place: Monocular regression of 3d people in depth. In *Proceedings of the IEEE/CVF Conference on Computer Vision and Pattern Recognition*, pages 13243–13252, 2022. 2
- [58] Sourabh Vora, Alex H Lang, Bassam Helou, and Oscar Beijbom. Pointpainting: Sequential fusion for 3d object detection. In *Proceedings of the IEEE/CVF conference on computer vision and pattern recognition*, pages 4604–4612, 2020. 1
- [59] Tuan-Hung Vu, Himalaya Jain, Maxime Bucher, Matthieu Cord, and Patrick Pérez. Advent: Adversarial entropy minimization for domain adaptation in semantic segmentation. In *Proceedings of the IEEE Conference on Computer Vision and Pattern Recognition*, pages 2517–2526, 2019. 3
- [60] Chunwei Wang, Chao Ma, Ming Zhu, and Xiaokang Yang. Pointaugmenting: Cross-modal augmentation for 3d object detection. In *Proceedings of the IEEE/CVF Conference on Computer Vision and Pattern Recognition*, pages 11794–11803, 2021. 1
- [61] Li Wang, Xinyu Zhang, Ziyang Song, Jiangfeng Bi, Guoxin Zhang, Haiyue Wei, Liyao Tang, Lei Yang, Jun Li, Caiyan Jia, et al. Multi-modal 3d object detection in autonomous driving: A survey and taxonomy. *IEEE Transactions on Intelligent Vehicles*, 2023. 1
- [62] Shihao Wang, Xiaohui Jiang, and Ying Li. Focal-petr: Embracing foreground for efficient multi-camera 3d object detection. *arXiv preprint arXiv:2212.05505*, 2022. 3
- [63] Shuo Wang, Xinhai Zhao, Hai-Ming Xu, Zehui Chen, Dameng Yu, Jiahao Chang, Zhen Yang, and Feng Zhao. Towards domain generalization for multi-view 3d object detection in bird-eye-view. In *Proceedings of the IEEE/CVF Conference on Computer Vision and Pattern Recognition*, pages 13333–13342, 2023. 1
- [64] Tai Wang, Qing Lian, Chenming Zhu, Xinge Zhu, and Wenwei Zhang. Mv-fcos3d++: Multi-view camera-only 4d object detection with pretrained monocular backbones. *arXiv preprint arXiv:2207.12716*, 2022. 2
- [65] Wen Wang, Yang Cao, Jing Zhang, Fengxiang He, Zheng-Jun Zha, Yonggang Wen, and Dacheng Tao. Exploring sequence feature alignment for domain adaptive detection transformers. In *Proceedings of the 29th ACM International Conference on Multimedia*, pages 1730–1738, 2021. 6, 7
- [66] Yue Wang, Vitor Campagnolo Guizilini, Tianyuan Zhang, Yilun Wang, Hang Zhao, and Justin Solomon. Detr3d: 3d object detection from multi-view images via 3d-to-2d queries. In *Conference on Robot Learning*, pages 180–191. PMLR, 2022. 3
- [67] Yingjie Wang, Qiuyu Mao, Hanqi Zhu, Jiajun Deng, Yu Zhang, Jianmin Ji, Houqiang Li, and Yanyong Zhang. Multi-modal 3d object detection in autonomous driving: a survey. *International Journal of Computer Vision*, pages 1–31, 2023. 1
- [68] Garrett Wilson and Diane J Cook. A survey of unsupervised deep domain adaptation. *ACM Transactions on Intelligent Systems and Technology (TIST)*, 11(5):1–46, 2020. 1
- [69] Enze Xie, Zhiding Yu, Daquan Zhou, Jonah Philion, Anima Anandkumar, Sanja Fidler, Ping Luo, and Jose M Alvarez. M² bev: Multi-camera joint 3d detection and segmentation with unified birds-eye view representation. *arXiv preprint arXiv:2204.05088*, 2022. 2
- [70] Kaixin Xiong, Shi Gong, Xiaoqing Ye, Xiao Tan, Ji Wan, Errui Ding, Jingdong Wang, and Xiang Bai. Cape: Camera view position embedding for multi-view 3d object detection. 2023. 1, 3
- [71] Jianyun Xu, Ruixiang Zhang, Jian Dou, Yushi Zhu, Jie Sun, and Shiliang Pu. Rpvnet: A deep and efficient range-point-voxel fusion network for lidar point cloud segmentation. In *Proceedings of the IEEE/CVF International Conference on Computer Vision*, pages 16024–16033, 2021. 1

- [72] Runsheng Xu, Zhengzhong Tu, Hao Xiang, Wei Shao, Bolei Zhou, and Jiaqi Ma. Cobevt: Cooperative bird's eye view semantic segmentation with sparse transformers. *arXiv preprint arXiv:2207.02202*, 2022. [3](#)
- [73] Chenyu Yang, Yuntao Chen, Hao Tian, Chenxin Tao, Xizhou Zhu, Zhaoxiang Zhang, Gao Huang, Hongyang Li, Yu Qiao, Lewei Lu, et al. Bevformer v2: Adapting modern image backbones to bird's-eye-view recognition via perspective supervision. In *Proceedings of the IEEE/CVF Conference on Computer Vision and Pattern Recognition*, pages 17830–17839, 2023. [1](#), [3](#)
- [74] Weixiang Yang, Qi Li, Wenxi Liu, Yuanlong Yu, Yuexin Ma, Shengfeng He, and Jia Pan. Projecting your view attentively: Monocular road scene layout estimation via cross-view transformation. In *Proceedings of the IEEE/CVF conference on computer vision and pattern recognition*, pages 15536–15545, 2021. [3](#)
- [75] Tianwei Yin, Xingyi Zhou, and Philipp Krahenbuhl. Center-based 3d object detection and tracking. In *Proceedings of the IEEE/CVF conference on computer vision and pattern recognition*, pages 11784–11793, 2021. [1](#)
- [76] Jin Hyeok Yoo, Yecheol Kim, Jisong Kim, and Jun Won Choi. 3d-cvf: Generating joint camera and lidar features using cross-view spatial feature fusion for 3d object detection. In *Computer Vision–ECCV 2020: 16th European Conference, Glasgow, UK, August 23–28, 2020, Proceedings, Part XXVII 16*, pages 720–736. Springer, 2020. [1](#)
- [77] Jinze Yu, Jiaming Liu, Xiaobao Wei, Haoyi Zhou, Yohei Nakata, Denis Gudovskiy, Tomoyuki Okuno, Jianxin Li, Kurt Keutzer, and Shanghang Zhang. Mtrans: Cross-domain object detection with mean teacher transformer. In *European Conference on Computer Vision*, pages 629–645. Springer, 2022. [6](#), [7](#)
- [78] Pan Zhang, Bo Zhang, Ting Zhang, Dong Chen, Yong Wang, and Fang Wen. Prototypical pseudo label denoising and target structure learning for domain adaptive semantic segmentation. In *Proceedings of the IEEE/CVF conference on computer vision and pattern recognition*, pages 12414–12424, 2021. [3](#)
- [79] Qiming Zhang, Jing Zhang, Wei Liu, and Dacheng Tao. Category anchor-guided unsupervised domain adaptation for semantic segmentation. In *Advances in Neural Information Processing Systems*, pages 433–443, 2019. [3](#)
- [80] Youshan Zhang. A survey of unsupervised domain adaptation for visual recognition. *arXiv preprint arXiv:2112.06745*, 2021. [1](#)
- [81] Yunpeng Zhang, Zheng Zhu, Wenzhao Zheng, Junjie Huang, Guan Huang, Jie Zhou, and Jiwen Lu. Beverage: Unified perception and prediction in birds-eye-view for vision-centric autonomous driving. *arXiv preprint arXiv:2205.09743*, 2022. [2](#)
- [82] Qinqing Zhao. A survey on virtual reality. *Science in China Series F: Information Sciences*, 52(3):348–400, 2009. [1](#)
- [83] Brady Zhou and Philipp Krähenbühl. Cross-view transformers for real-time map-view semantic segmentation. In *Proceedings of the IEEE/CVF conference on computer vision and pattern recognition*, pages 13760–13769, 2022. [5](#), [6](#)
- [84] Jinjing Zhu, Haotian Bai, and Lin Wang. Patch-mix transformer for unsupervised domain adaptation: A game perspective. In *Proceedings of the IEEE/CVF Conference on Computer Vision and Pattern Recognition (CVPR)*, pages 3561–3571, June 2023. [1](#)
- [85] Xinge Zhu, Hui Zhou, Tai Wang, Fangzhou Hong, Yuexin Ma, Wei Li, Hongsheng Li, and Dahua Lin. Cylindrical and asymmetrical 3d convolution networks for lidar segmentation. In *Proceedings of the IEEE/CVF conference on computer vision and pattern recognition*, pages 9939–9948, 2021. [1](#)
- [86] Jiayu Zou, Junrui Xiao, Zheng Zhu, Junjie Huang, Guan Huang, Dalong Du, and Xingang Wang. Hft: Lifting perspective representations via hybrid feature transformation. *arXiv preprint arXiv:2204.05068*, 2022. [3](#)
- [87] Yang Zou, Zhiding Yu, BVK Kumar, and Jinsong Wang. Unsupervised domain adaptation for semantic segmentation via class-balanced self-training. In *Proceedings of the European conference on computer vision (ECCV)*, pages 289–305, 2018. [5](#)